ORIGINAL RESEARCH

Antimicrobial and Cytotoxic Effect of *Bornetella Nitida* Green Algae Isolate on MCF-7 Breast Cancer

Yuni Elsa Hadisaputri [1], Nunuk Hariani Soekamto[2], Pratiwi Pudjiastuti [3], Aria Aristokrat [1], Bahrun Bahrun[2,4], Fajar Fauzi Abdullah[5], Tatsufumi Okino[4]

[1]Department of Pharmaceutical Biology, Faculty of Pharmacy, Universitas Padjadjaran, Jatinangor, West Java, 45363, Indonesia; [2]Department of Chemistry, Faculty of Mathematics and Natural Sciences, Hasanuddin University, Makassar, Indonesia; [3]Department of Chemistry, Faculty of Mathematics and Natural Sciences, Airlangga University, Surabaya, Indonesia; [4]Faculty of Environmental Earth Science, Hokkaido University, Hokkaido, Japan; [5]Department of Chemistry, Faculty of Mathematics and Natural Sciences, Universitas Garut, Kabupaten Garut, Indonesia

Correspondence: Yuni Elsa Hadisaputri, Department of Pharmaceutical Biology, Faculty of Pharmacy, Universitas Padjadjaran, Jl. Raya Bandung-Sumedang KM.21, Jatinangor, West Java, 45363, Indonesia, Tel +62-22-84288888, Email yuni.elsa@unpad.ac.id

Introduction: Marine algae are increasingly becoming a potential resource for new drugs. In recent decades, including *Bornetella nitida* (*B. nitida*). Meanwhile, antimicrobial and anticancer agents are the first line of choice for developing alternative compounds, considering the annually increasing resistant events. Therefore, this study aimed to examine the antimicrobial and cytotoxic potential of *B. nitida* isolate compounds.

Methods: The *B. nitida* resulted in 2 compounds, sitosterol 3β tetracosanoate and (E)-17-(8-ethyl-4,5,9-trimethyldec-6-en-2-yl)-13-methyl-2,3,4,7,8,9,10,11,12,13,14,15,16,17-tetradecahydro-1H-cyclopenta[a]phenanthren-3-ol. Both compounds were tested to have antibacterial effects against *Pseudomonas aeruginosa*, *Bacillus subtilis*, *Staphylococcus aureus*, *Methicillin-resistant Staphylococcus Aureus* (MRSA). Proliferation assay was conducted using the PrestoBlue™ Cell Viability Reagent, which was also used to measure the IC_{50} against MCF-7 breast cancer cells.

Results: The results showed that (E)-17-(8-ethyl-4,5,9-trimethyldec-6-en-2-yl)-13-methyl-2,3,4,7,8,9,10,11,12,13,14,15,16,17-tetradecahydro-1H-cyclopenta[a]phenanthren-3-ol had antimicrobial activity against *Staphylococcus aureus* and IC_{50} value of 142.18 μg/mL against MCF-7 cells, while sitosterol 3β tetracosanoate does not have any antimicrobial activity and IC_{50} value of 681.65 μg/mL. Moreover, the mechanism prediction using docking with caspase-3 receptor to induce apoptosis was also evaluated.

Conclusion: Based on the results, (E)-17-(8-ethyl-4,5,9-trimethyldec-6-en-2-yl)-13-methyl-2,3,4,7,8,9,10,11,12,13,14,15,16,17-tetradecahydro-1H-cyclopenta[a]phenanthren-3-ol of *B. nitida* has great potential as an antimicrobial and anticancer agent.

Keywords: *Bornetella nitida*, *Staphylococcus aureus*, MCF-7, cytotoxic, apoptosis

Introduction

Drug discovery and development for antibiotics and anticancer are currently the most urgent study topics.[1] Infection diseases have become an important topic during pandemics. The invention of antibiotics is expected to solve infectious disease problems that need fast solutions.[2] Breast Cancer occurrence worldwide increased rapidly and became the highest cancer incidence in the Global Cancer Observatory (GLOBOCAN) 2022 report.[3] Almost 80% of breast cancer that is reported is ER positive type.[4]

Recent studies are competing to find new compounds not only from traditional and rare land plants but also from marine sources. Marine environment covers about 75% of the total Earth's surface, comprising about half of the total global biodiversity. Algae are promising sources of various bioactive compounds, with a diverse group in the habitat.[5] Both micro and macroalgae contain various novel bioactive compounds with antimicrobial agent, cytotoxic properties, and antiviral activity.[6]

Bornetella nitida (*B. nitida*), which belongs to the class Ulvophyceae or Ulvophytes called sea lettuce and order Dasycladales is unicellular green algae. Various forms of green algae have been reported. For example, *Chaetomorpha bracyhygona* contain dichloacetic, oximes, and L-α-Terpinol as cytotoxic agent (SiHa cells, IC_{50}: 23.6 µg/mL),[6] while *Caulerpa lentifera* is used for antiobesity (EC_{50}: 92,11–114.3 µg/mL), and is cytotoxic (100.50–7080.00 µg/mL).[7] *Ulva rigida* contains fatty acids that reportedly have antimicrobial activity against *Staphylococcus aureus* and *Enterococcus faecalis,* with an inhibition diameter of 16.3–23 mm at a concentration of 250 µg/mL.[8] Our previous reported *B. nitida* *n*-hexane extract has activity as antioxidant 22.20 µg/mL and *B. nitida* ethyl acetate extract cytotoxic activity against HeLa cells with an IC_{50} of 281.09 µg/mL.[9]

There are currently no studies on the use of green algae *B. nitida* for antimicrobial or anticancer. Therefore, this study aimed to examine the antimicrobial potential of *B. nitidia* isolate compounds using in vitro and in silico approaches.

## Material and Methods

Bornetella Nitida Green Algae

B. nitida green algae were obtained from the Selayar Island Sea when water conditions have receded (Figure 1). Morphological and taxonomic analyses were performed at the Indonesian Institute of Sciences, Oceanography Laboratory (specimen code 1346–34,232-1). *B. nitida* was dried and made into powder for subsequent analysis.

Bornetella Nitida Isolation

B. nitida powder weighing 4.8 kg was extracted through a multistage maceration method using *n*-hexane, chloroform, ethyl acetate, and methanol. For compound 1, 19.81 grams of *n*-hexane extract was fractionated using vacuum column chromatography. Seven combined fractions were obtained through the initial fractionation. The H2 fraction was further fractionated by compressed and gravity column chromatography to obtain a pure compound in the form of a white powder (compound 1), with the isolation method shown in Figure 2A. Compound 2 obtained from 4.94 grams of the ethyl acetate extract was fractionated using vacuum column chromatography (VLC), resulting in 10 combined fractions. Each fraction was further fractionated using chromatographic methods, as described previously. The fractionation results produced one compound from the E3 fraction and the extraction method is illustrated in Figure 3A.

Compounds 1 and 2 Determinations

Fourier transform infrared spectroscopy (FTIR) spectra were recorded on a SHIMADZU IR Prestige-21 in KBr using an NMR JEOL ECZ-500 and Varian Unity INO-VA-500 Spectrometer (Agilent Technologies, Santa Carla, CA, USA). NMR data were recorded at 500 MHz for 1H and 125 MHz for 13C using TMS as the internal standard. Furthermore,
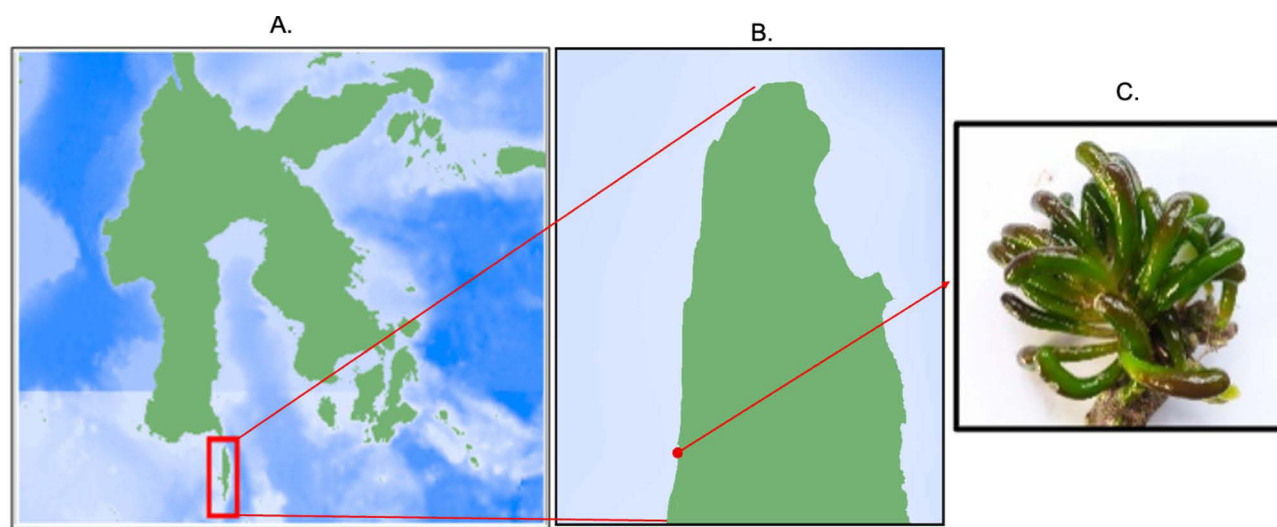
Figure 1 *B. nitida* sampling location at Selayar Island Sea. (**A**) Sampling location on the island of Sulawesi, Indonesia. (**B**) Selayar Island Sea coordinate point 5°53'56.52"LS and 120°27'3.49"BT. (**C**) *B. nitidia* from Selayar Island Sea.

A.

B.
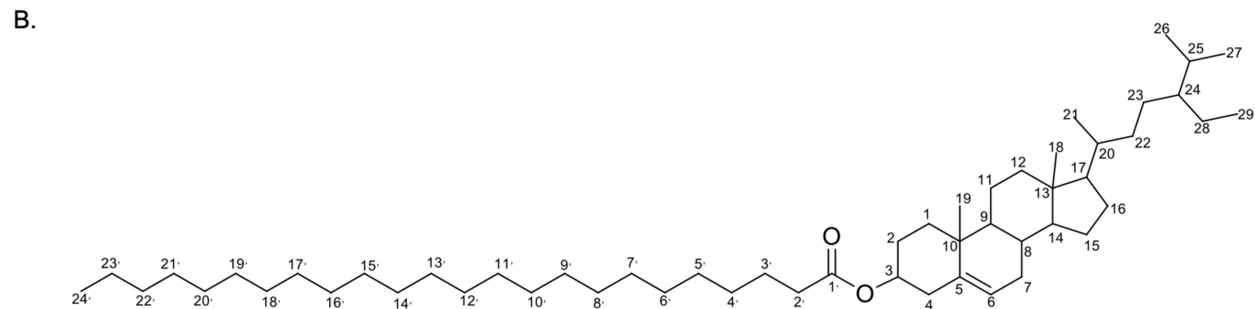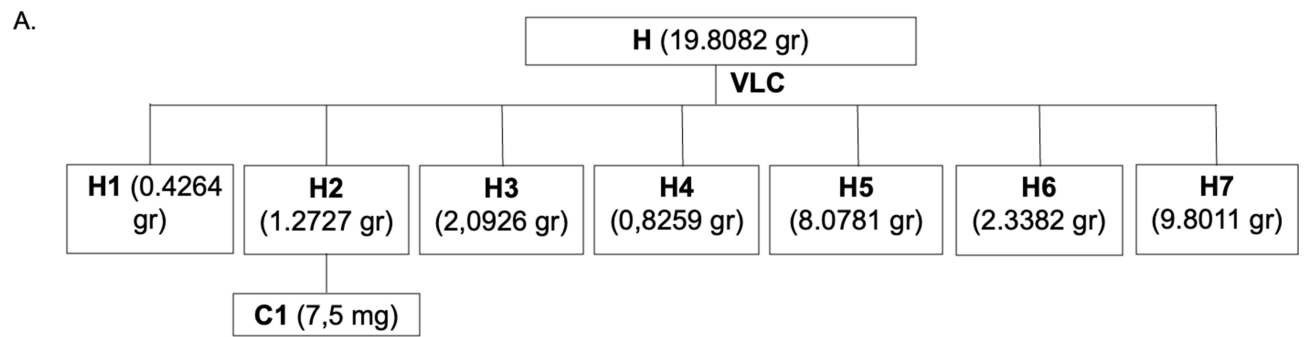
Figure 2 Compound 1, sitosterol 3β tetracosanoate. (**A**) Compound 1 obtained from *n*-Hexane extract of *B. nitida* with Vacuum liquid chromatography (VLC) method process. (**B**) Structure of compound 1, sitosterol 3β tetracosanoate.

A.

B.
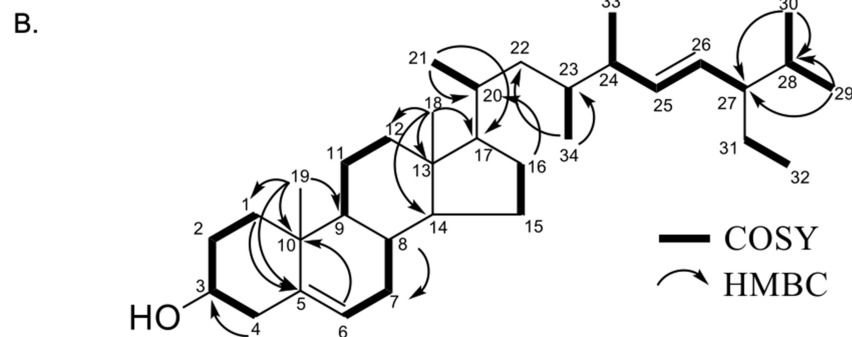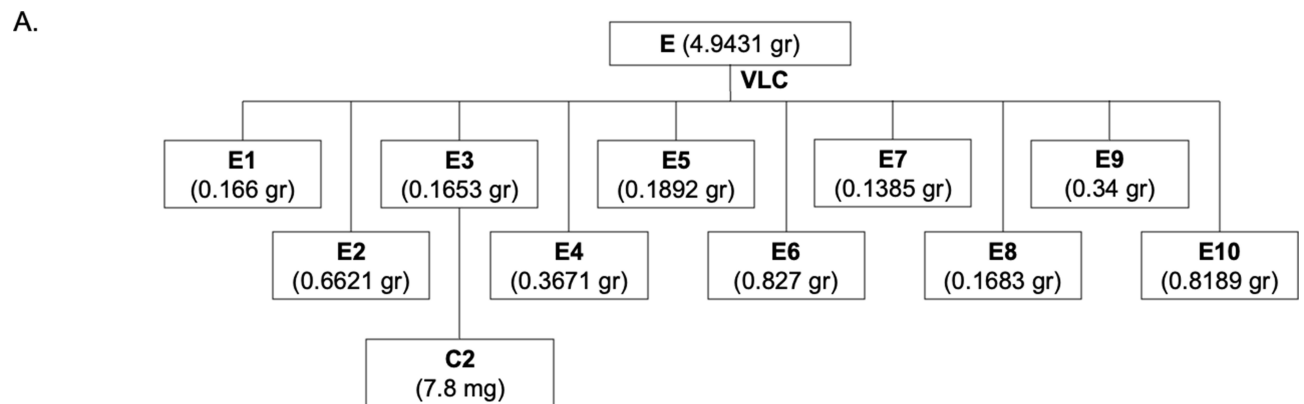
Figure 3 Compound 2, (E)-17-(8-ethyl-4,5,9-trimethyldec-6-en-2-yl)-13-methyl-2,3,4,7,8,9,10,11,12,13,14,15,16,17-tetradecahydro-1H-cyclopenta[a]phenanthren-3-ol. (**A**) Compound 2 obtained from ethyl acetate extract of *B. nitida* with vacuum liquid chromatography (VLC) method process. (**B**) Structure of compound 2,(E)-17-(8-ethyl-4,5,9-trimethyldec-6-en-2-yl)-13-methyl-2,3,4,7,8,9,10,11,12,13,14,15,16,17-tetradecahydro-1H-cyclopenta[a]phenanthren-3-ol.

column chromatography was conducted on silica gel 60 (70–230 and 230–400 mesh, Merck), after which a TLC analysis was carried out on 60 GF254 (Merck, 0.25 mm) using various solvent systems to detect spots by irradiation under ultraviolet-visible light (257 and 364 nm) and heating silica gel plates sprayed with H_2SO_4 in EtOH (10%).

Bacteria Culture and Antimicrobial Test

Bacteria used in this study including *Pseudomonas aeruginosa* (*P. aeruginosa*) (ATCC 9027), *Bacillus subtilis* (*B. subtilis*) (ATCC 6633), *Staphylococcus aureus* (*S. aureus*) (ATCC 6538), and *Methicillin-Resistant Staphylococcus aureus (MRSA)* (ATCC BAA-44) were obtained from American Type Culture Collection (ATCC). Soybean-Casein Digest Agar (Himedia, Thane, India) was used for this antimicrobial testing. For antimicrobial control, 10 μg Methicillin MET (Himedia, India), 5 μg ciprofloxacin (Himedia, India), and 15 μg rifampicin (Himedia, India) were used. Serial dilutions of compounds 1 and 2 at concentrations of 250, 500, 750, and 1000 μg/mL were used in the antibiotic potency test. Antimicrobial test was done on three replications.

Culture Cell Lines

The breast adenocarcinoma cells MCF-7 were obtained from the European Collection of Authenticated Cell Cultures (ECACC), then cultured in Eagle's Minimum Essential Medium (EMEM) (Sigma Aldrich; Merck KGaA, Darmstadt, Germany) supplemented with 10% fetal bovine serum (Sigma Aldrich; Merck KGaA), 100 U/mL penicillin, and 100 μg/ mL streptomycin (Sigma Aldrich; Merck KGaA). Cells were cultured in a CO_2 incubator with 5% CO_2 at 37°C. The medium was replaced once every 2 days. Cell and cell conditions were checked daily using an inverted microscope (Axio Vert.A1, Zeiss, Oberkochen, Baden-Württemberg, Germany).

Cell Proliferation Test

The cytotoxicity of *B. nitida* compounds 1 and 2 was tested in an MCF-7 breast cancer cell line. The tests used a permeable resazurin-based solution that functioned as a cell viability indicator, using the reducing power of living cells to quantitatively measure proliferation. Cell viability was determined using the PrestoBlue™ Cell Viability Reagent (Thermo Fisher Scientific Inc., Waltham, Massachusetts, USA) according to the manufacturer's instructions. The concentrations of compounds 1 and 2 were 7.8, 15.6, 31.25, 62.5, 125, and 250 μg/mL. Cisplatin was used as a positive control in this test. Cell suspensions (50 μL; 1×10^4 cells) were added to each well of a 96-well plate (Falcon, Franklin Lakes, NJ, USA) and incubated at 37°C for 24 h. The absorbance was read at 560 nm reference 615 nm using an Infinite M200 PRO microplate reader (Tecan, Männedorf, Switzerland). The cell proliferation inhibition (CPI) rate (%) was calculated using the following formula: CPI rate (%) = (1-OD490 of untreated cells) × 100. Proliferation test was done on three replications.

Molecular Docking of Compounds 1 and 2 in Caspase-3 Active Site

An Acer Swift SF314-56G running Windows 11 Home Single Language 64-bit and equipped with an Intel® CoreTM i5-8265U CPU and 4.00 GB of RAM was the PC used in this experiment. The Biovia Discovery Studio Visualizer was used to visualize the docking positions and interactions. AutoDock 1.5.6 was used for the synthesis of macromolecules and ligands as well as the performance of docking investigations.

Ligand Preparation

Compounds 1 and 2 were drawn with ChemDraw 20.1.1, and energy was minimized using Chem3D 20.1.1, then stored in *pdb format. A Gasteiger load was added to the test ligand by using AutoDock. In addition, the ligands automatically adjust the non-polar merge such that only the polar H atom is expected to interact with the protein residues. The lowest energy value of the ligand was selected because the compound in the original form would occur spontaneously. Subsequently, a torsion tree was constructed to observe the rigid and flexible parts of the compound. All ligand files were saved in *pdbqt format.

Receptor Preparation

BIOVIA Discovery Studio was used to visualize the caspase-3 3D structure from the Protein Data Bank (PDB ID:

1NME). Subsequently, the water molecules surrounding the protein were eliminated along with those components, separating the protein chain from the native ligand. The receptor in PDB file format represents the structure created. Furthermore, by removing the protein chain, the structure of the native ligand was restored and stored in an * PDB file format. Proteins and native ligands were produced using AutoDockTools 1.5.6 software. This requires the addition of hydrogen atoms to the polar side of the structure, application of Kollman charges for the receptor, and Gasteiger charges for the native ligand.

Validation of the Molecular Docking Method

The method was tested to ensure that the docking parameters were suitable for docking the test ligand with the caspase-3 receptor. To perform this validation, re-docking was performed, which entailed the re-introduction of the dissociated native ligand into the caspase-3 receptor. The re-docking process used a grid box of 30×30×30, with coordinates x = 42.233, y = 96.971, and z = 24.375. In the docking settings, Lamarckian genetic algorithm (GA) 4.2 was used as the docking strategy, and the values were set to 100. Default was used for all other docking options and one parameter to consider from the re-docking results was the Root Mean Square Deviation (RMSD) with an acceptable value of 2.0.

Molecular Docking

After optimization and production, compounds 1 and 2 were docked to the caspase-3 receptor. The receptor was developed by docking in the same manner as in the method validation after separation from the native ligand using AutoDockTools 1.5.6.

Data Analysis and Visualization

The data presentation design in this study considered several variables, including the number of hydrogen bonds, van der Waals bonds, conventional hydrogen bonds, and binding free energy. Both two-dimensional (2D) and three-dimensional (3D) representations of the receptor complex conformations, ligand interactions, and contact amino acid residues were achieved using the BIOVIA Discovery Studio.
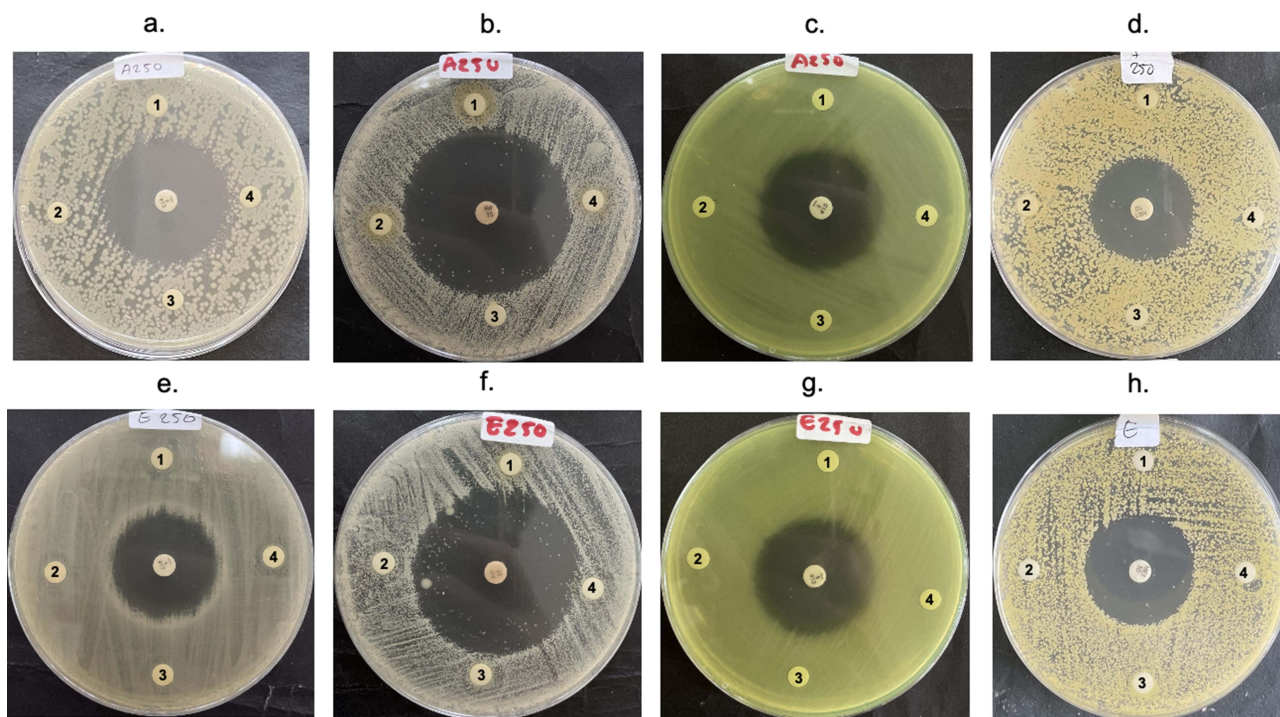
Results
Compounds 1 and 2 Determination

Compound 1 was obtained as a white amorphous solid and the TOF-MS spectrum shows [M+H]+ m/z 679.6013 (calculated $C_{47}H_{82}O_2$, m/z 678.6388) and a fragment ion peak at m/z 415.2132 [M+H-265], indicating the loss of a fatty acid (n-tetracosanoic acid unit). This corresponds to the molecular formula $C_{29}H_{50}O$, requiring five degrees of unsaturation originating from a pair of C sp^2 and the remaining tetracyclic steroid stigmastane type. The IR spectrum shows absorption peaks at 3,424 cm^{-1} (OH), 2,937 and 2,870 cm^{-1} (C-H sp^3), 1464 cm^{-1} (C=C), 1379 cm^{-1} (gem-dimethyl group), and 1056 cm^{-1} (CO). Furthermore, the 1H-NMR spectrum (CDCl$_3$ 500 MHz) shows the presence of six methyl groups, including two tertiary resonating at δH 1.02 (CH$_3$-19) and 0.67 (CH$_3$-19), three secondary resonating at δH 0.92 (3H, d, J = 6.7 Hz, CH$_3$-21), 0.83 (3H, m, CH$_3$-26), and 0.82 (3H, m, CH$_3$−27), as well as one primary at δH 0.84 (3H m, CH$_3$-29), indicating the presence of a stigmastane-type steroid skeleton. One methine olefin group resonates at δH 5.37 (d, J = 5.0 Hz, H-6) and the oxymethine group resonates at δH 4.62 (1H, td, J = 10.2; 9.2; 4.3 Hz H-3). The chemical shift of the proton is greater because in this position there is an ester bridge from the carbonyl, which binds to the fatty acid. Moreover, fatty acids were observed in the 1H NMR spectrum, which resonated overlapping in the δH range of 1.25–2.26 ppm. The 13C-NMR (CDCl$_3$ 150 MHz) and DEPT 135° spectra showed the presence of six methyl groups, including one olefinic methine, one olefinic quaternary carbon, and an oxygenated methine group resonating at δC 73.8 (C-3); indicating the presence of a stigmastane type steroid.[10–12]

Potency Antimicrobial Activity of sitosterol 3β tetracosanoate and (E)-17-(8-ethyl-4,5,9-trimethyldec-6-en-2-yl)-13-methyl-2,3,4,7,8,9,10,11,12,13,14,15,16,17-tetradecahydro-1H-cyclopenta[a]phenanthren-3-ol

The antibiotic potency test results showed that sitosterol 3β tetracosanoate did not have potent antimicrobial activity against *S. aureus, B. subtilis, P. aeruginosa*, and MRSA as shown in Figure 4a–d. Meanwhile, (E)-17-(8-ethyl-4,5,9-trimethyldec-6-en-2-yl)-13-methyl-2,3,4,7,8,9,10,11,12,13,14,15,16,17-tetradecahydro-1H-cyclopenta[a]

Figure 4 Bacteria inhibition test results for sitosterol 3β tetracosanoate and (E)-17-(8-ethyl-4,5,9-trimethyldec-6-en-2-yl)-13-methyl-2,3,4,7,8,9,10,11,12,13,14,15,16,17-tetradecahydro-1H-cyclopenta[a]phenanthren-3-ol. (**a**) sitosterol 3β tetracosanoate against *S. aureus*, (**b**) *B. subtilis*, (**c**) *P. aeruginosa*, (**d**) and MRSA. (**e**) (E)-17-(8-ethyl-4,5,9-trimethyldec-6-en-2-yl)-13-methyl-2,3,4,7,8,9,10,11,12,13,14,15,16,17-tetradecahydro-1H-cyclopenta[a]phenanthren-3-ol against *S. aureus*, (**f**) *B. subtilis, P aeruginosa*, (**h**) and MRSA. Serial dilutions of compounds 1 and 2 at concentrations of [1]250,[2]500,[3]750, and[4]1000 μg/mL.

phenanthren-3-ol showed an inhibition area of 9.7, 10.5, 10.6, and 10.75 mm for 250, 500, 750, and 1000 μg/mL, respectively, against *S. aureus* (Figure 4e), but not in other bacteria (Figure 4f–h).
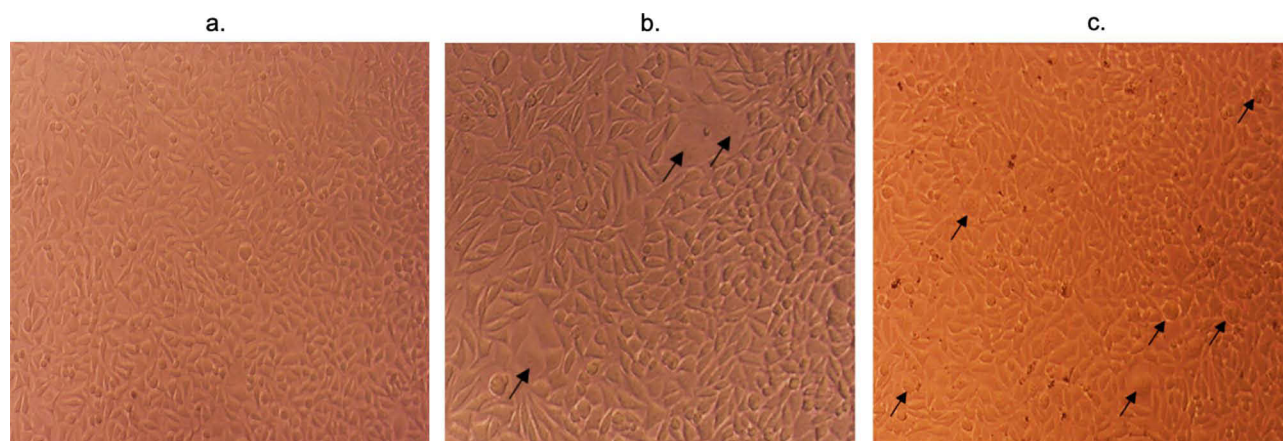
Cytotoxic Activity and Morphological Changes of sitosterol 3β tetracosanoate and (E)-17-(8-ethyl-4,5,9-tri-methyldec-6-en-2-yl)-13-methyl-2,3,4,7,8,9,10,11,12,13,14,15,16,17-tetradecahydro-1H-cyclopenta[a]phenanth-ren-3-ol

The IC$_{50}$ value results of sitosterol 3β tetracosanoate and (E)-17-(8-ethyl-4,5,9-trimethyldec-6-en-2-yl)-13-methyl-2,3,4,7,8,9,10,11,12,13,14,15,16,17-tetradecahydro-1H-cyclopenta[a]phenanthren-3-ol are 681.65 and 142.18 μg/mL, respectively, as shown in Table 1. The morphology results showed apoptotic process occurrence in MCF-7 cells photographs 24 h after

Table 1 Cytotoxic and Antimicrobial Activity of the Isolated Compounds from *B. Nitida*

Compund	IC$_{50}$ against MCF-7 cell lines (μg/mL)	Inhibition zone (mm)			
		S. aureus	*B. subtilis*	*P. aeruginosa*	**MRSA**
Sitosterol 3β tetracosanoate	681.65	ND	ND	ND	ND
(E)-17-(8-ethyl-4,5,9-trimethyldec-6-en-2-yl)-13-methyl-2,3,4,7,8,9,10,11,12,13,14,15,16,17-tetradecahydro-1H-cyclopenta[a]phenanthren-3-ol	142.18	10.7	ND	ND	ND
Cisplatin	49.25	-	-	-	-
Ciprofloxacin	-	37.84	-	30.2	-
Rifampicin	-	-	25.9	-	-
Methicillin	-	-	-	-	27.7

Notes: Measured as radius of inhibition from edge of disk impregnated with 1000 μg/mL of test compound. ND = not detected.

Figure 5 Photograph of MCF-7 cells morphology, (**a**) untreated, (**b**) treated with sitosterol 3β tetracosanoate, and (**c**) treated with (E)-17-(8-ethyl-4,5,9-trimethyldec-6-en-2-yl)-13-methyl-2,3,4,7,8,9,10,11,12,13,14,15,16,17-tetradecahydro-1H-cyclopenta[a]phenanthren-3-ol. Black arrow showed the blebbing sign that the apoptosis process is going on.

treatment with sitosterol 3β tetracosanoate and (E)-17-(8-ethyl-4,5,9-trimethyldec-6-en-2-yl)-13-methyl-2,3,4,7,8,9,10,11,12,13,14,15,16,17-tetradecahydro-1H-cyclopenta[a]phenanthren-3-ol. Blebbing and rupture occurred in MCF-7 cells, as shown by the black arrows, with (E)-17-(8-ethyl-4,5,9-trimethyldec-6-en-2-yl)-13-methyl-2,3,4,7,8,9,10,11,12,13,14,15,16,17-tetradecahydro-1H-cyclopenta[a]phenanthren-3-ol having more events than sitosterol 3β tetracosanoate (Figure 5).

Validation of the Molecular Docking Method

Based on the validation results, an RMSD value of 1.1 Å was obtained as shown in Table 2. Figure 6 shows 2D and 3D visualizations of the interactions between caspase-3 and the natural ligand. Conventional hydrogen bonds, van der Waals bonds, Pi-sulfur linkages, and Pi–Pi T-shaped connections were found as interactions between the ligand and caspase-3.

Molecular Docking of sitosterol 3β tetracosanoate and (E)-17-(8-ethyl-4,5,9-trimethyldec-6-en-2-yl)-13-methyl-2,3,4,7,8,9,10,11,12,13,14,15,16,17-tetradecahydro-1H-cyclopenta[a]phenanthren-3-ol in Caspase-3

Molecular docking was performed using native ligands, comparative drugs (sorafenib), sitosterol 3β tetracosanoate, and (E)-17-(8-ethyl-4,5,9-trimethyldec-6-en-2-yl)-13-methyl-2,3,4,7,8,9,10,11,12,13,14,15,16,17-tetradecahydro-1H-cyclopenta[a]phenanthren-3-ol, with caspase-3 (PDB ID: 1NME). Table 3 shows the energy binding values, inhibition constants, and binding to amino acids. (E)-17-(8-ethyl-4,5,9-trimethyldec-6-en-2-yl)-13-methyl-2,3,4,7,8,9,10,11,12,13,14,15,16,17-tetradecahydro-1H-cyclopenta[a]phenanthren-3-ol had the lowest binding energy value of −6.65 kcal/mol, lower than that of the natural ligand, at −5.00 kcal/mol, while (E)-17-(8-ethyl-4,5,9-trimethyldec-6-en-2-yl)-13-methyl-2,3,4,7,8,9,10,11,12,13,14,15,16,17-tetradecahydro-1H-cyclopenta[a]phenanthren-3-ol had the lowest inhibition constant (13.46 μM). Figure 7 shows the 2D and 3D visualizations of the interactions between caspase-3 with sitosterol 3β tetracosanoate and (E)-17-(8-ethyl-

Table 2 The Results of the Method Validation Through Re-Docking with 2-Hydroxy-5-(2-Mercapto-Ethylsulfamoyl)-Benzoic Acid

PDB ID	Grid Box (x, y, z)	Validation		Binding Energy (kcal/mol)
		RMSD cluster (Å)	**RMSD reference** (Å)	
1NME	42.233 96.971 24.375	0.00	1.1	−5.00
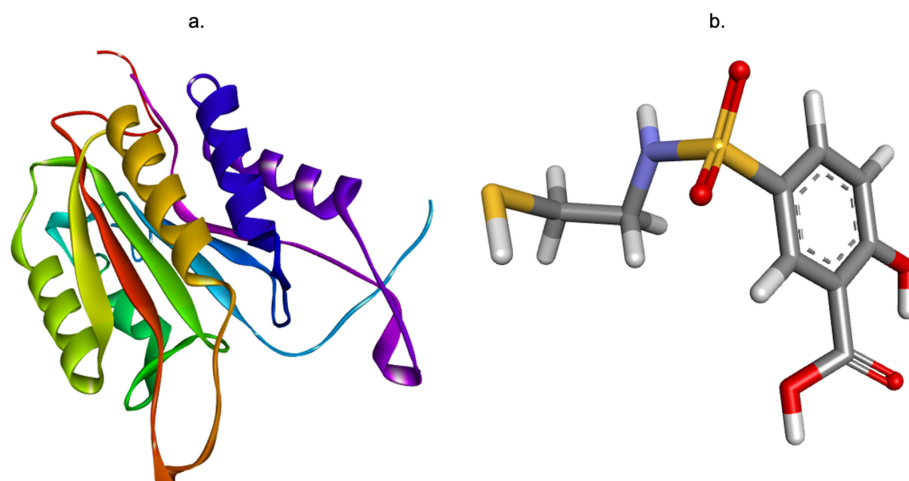
Figure 6 The three-dimensional (3D) structure of (**a**) caspase-3 without a ligand and (**b**) native ligand 2-Hydroxy-5-(2-mercapto-ethylsulfamoyl)-benzoic acid.

4,5,9-trimethyldec-6-en-2-yl)-13-methyl-2,3,4,7,8,9,10,11,12,13,14,15,16,17-tetradecahydro-1H-cyclopenta[a]phenanthren-3-ol.

Discussion

In this study, *B. nitida*, a large, unicellular, green marine macro algae, was obtained from the Selayar Island sea (Figure 1),[13] dried, powdered, and extracted using a multi-macerated method with several solvent *n*-hexane and ethyl

Table 3 The Docking Results of Sitosterol 3β Tetracosanoate and (E)-17-(8-Ethyl-4,5,9-Trimethyldec-6-En-2-Yl)-13-Methyl -2,3,4,7,8,9,10,11,12,13,14,15,16,17-Tetradecahydro-1H-Cyclopenta[a]phenanthren-3-Ol Against the Caspase-3 Receptor

No.	Compound	Binding Energy (kcal/mol)	KI (µM)	Bonding with amino acids		
				Hydrogen bonds	Van der waals bonds	Other bonds
1	Native ligand	−5.00	214.46	ASN 208, TRP 214, TYR 204, SER65, ARG 207, PHE 250	–	TRP 206
2	Sorafenib	−5.97	42.26	ARG 207, PHE 250, PHE 252	HIS 121, THR 62, SER 249, ASN 208, TRP 217, TRP 206, SER 205	TYR 204, SER 251
3	sitosterol 3β tetracosanoate	+22.32	–	–	–	ARG 207, TYR 204, TRP 214, PHE 252, TRP 206, PHE 250
4	(E)-17-(8-ethyl-4,5,9-trimethyldec-6-en-2-yl)-13-methyl -2,3,4,7,8,9,10,11,12,13,14,15,16,17-tetradecahydro-1H-cyclopenta[a]phenanthren-3-ol	−6.65	13.46	GLU 248	-	TYR 204, TRP 206, ARG 207

Abbreviations: IC, inhibition concentration; FTIR, Fourier-transform infrared spectroscopy; NMR, nuclear magnetic resonance; TLC, thin layer chromatography; VLC, vacuum liquid chromatography; PDB, protein data bank; RMSD, root mean standard deviation; KI, inhibitor constant.

562

Breast Cancer: Targets and Therapy 2024:16
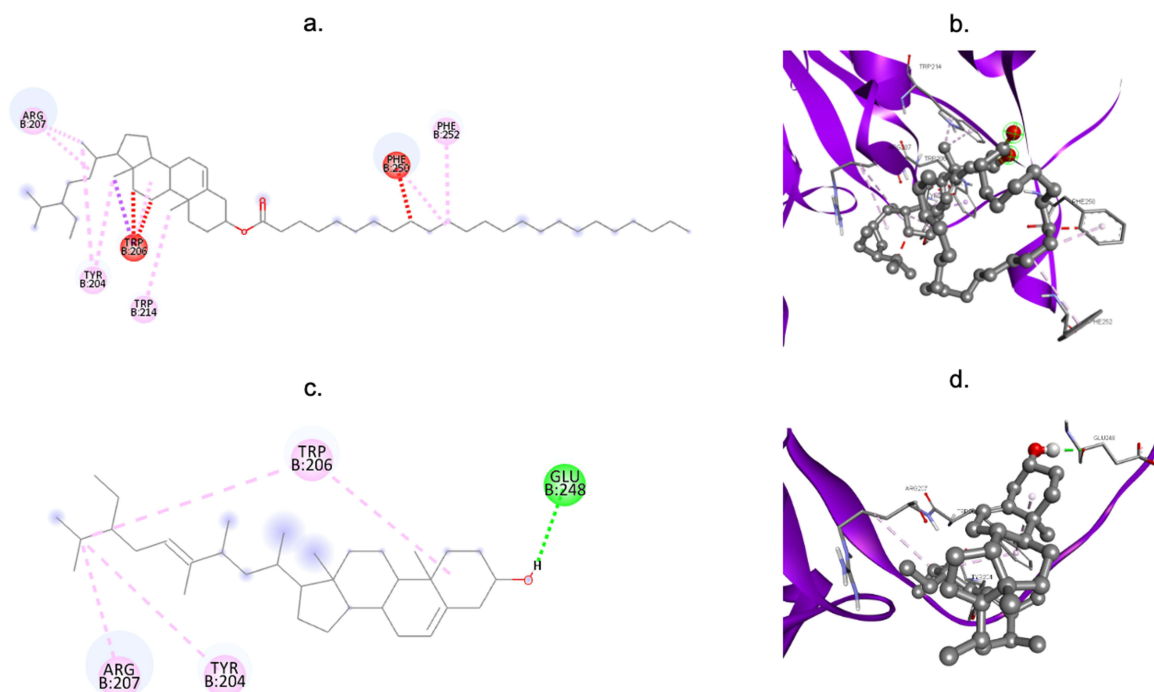
Figure 7 (**a**) Visualization of the 2D interactions between caspase-3 and sitosterol 3β tetracosanoate (**b**) and visualization of the 3D interactions between caspase-3 and sitosterol 3β tetracosanoate (**c**) Visualization of the 2D interactions between caspase-3 and (**E**)-17-(8-ethyl-4,5,9-trimethyldec-6-en-2-yl)-13-methyl -2,3,4,7,8,9,10,11,12,13,14,15,16,17-tetradecahydro-1H-cyclopenta[a]phenanthren-3-ol (**d**) and visualization of the 3D interactions between caspase-3 and (**E**)-17-(8-ethyl-4,5,9-trimethyldec-6-en-2-yl)-13-methyl-2,3,4,7,8,9,10,11,12,13,14,15,16,17-tetradecahydro-1H-cyclopenta[a]phenanthren-3-ol.

acetate (Figure 2A and 3A) to obtain compounds 1 and 2 (Figure 2B and 3B). After identification using NMR, compound 1 was identified as sitosterol 3β tetracosanoate, while compound 2 was found to be (E)-17-(8-ethyl-4,5,9-trimethyldec-6-en-2-yl)-13-methyl-2,3,4,7,8,9,10,11,12,13,14,15,16,17-tetradecahydro-1H-cyclopenta[a]phenanthren-3-ol.

Both compounds were tested against *P. aeruginosa, B. subtilis, S. aureus*, and MRSA (Figure 4). Based on the results, only (E)-17-(8-ethyl-4,5,9-trimethyldec-6-en-2-yl)-13-methyl-2,3,4,7,8,9,10,11,12,13,14,15,16,17-tetradecahydro-1H-cyclopenta[a] phenanthren-3-ol inhibited the growth of *S. aureus* with an inhibition zone 10.7 mm. Similarly, the proliferation assay showed that (E)-17-(8-ethyl-4,5,9-trimethyldec-6-en-2-yl)-13-methyl-2,3,4,7,8,9,10,11,12,13,14,15,16,17-tetradecahydro-1H-cyclopenta[a] phenanthren-3-ol has better activity in inhibiting the growth of MCF-7 cells with a smaller IC_{50} value, in the moderate category. Figure 5 presents the morphology of MCF-7 under microscope. MCF-7 cells exposed to (E)-17-(8-ethyl-4,5,9-trimethyldec-6-en-2-yl)-13-methyl-2,3,4,7,8,9,10,11,12,13,14,15,16,17-tetradecahydro-1H-cyclopenta[a]phenanthren-3-ol experience blebbing, an early sign of apoptosis or programmed death. Based on these results, the estimated interaction was simulated through docking (Table 2) by targeting caspase-3, a marker of apoptosis, as a target protein (Figure 6). As predicted, the molecular docking results of (E)-17-(8-ethyl-4,5,9-trimethyldec-6-en-2-yl)-13-methyl-2,3,4,7,8,9,10,11,12,13,14,15,16,17-tetradecahydro-1H-cyclopenta [a]phenanthren-3-ol showed the lowest binding energies (Table 3). The 2D and 3D interactions between caspase-3 and (E)-17-(8-ethyl-4,5,9-trimethyldec-6-en-2-yl)-13-methyl-2,3,4,7,8,9,10,11,12,13,14,15,16,17-tetradecahydro-1H-cyclopenta[a]phe-nanthren-3-ol are shown in Figure 7.

Green algae *B. nitida* contains steroids derivatives, and this study reports compound 1 as sitosterol 3β tetracosanoate (Figure 2) and compound 2 was (E)-17-(8-ethyl-4,5,9-trimethyldec-6-en-2-yl)-13-methyl-2,3,4,7,8,9,10,11,12,13,14,15,16,17-tetradecahydro-1H-cyclopenta[a]phenanthren-3-ol (Figure 3). According to previous studies, the green algae family contains fatty acids, chloroacetic acids, imines, or terpenoids.[6,8] This study completed an inventory of the contents of green algae, namely *B. nitida*.

The activity of sitosterol 3β tetracosanoate and (E)-17-(8-ethyl-4,5,9-trimethyldec-6-en-2-yl)-13-methyl -2,3,4,7,8,9,10,11,12,13,14,15,16,17-tetradecahydro-1H-cyclopenta[a]phenanthren-3-ol was investigated as antimicrobial agents against *P. aeruginosa, B. subtilis, S. aureus*, and MRSA (Figure 4). However, only (E)-17-(8-ethyl-4,5,9-tri-methyldec-6-en-2-yl)-13-methyl-2,3,4,7,8,9,10,11,12,13,14,15,16,17-tetradecahydro-1H-cyclopenta[a]phenanthren-3-ol inhibited the growth of *S. aureus* at a concentration 250 µg/mL with an inhibition diameter of about 9.7 mm. Another green algae, *Ulva rigida* was also reported to show antimicrobial activity against *S. aureus* and *Enterococcus faecalis* at the same concentration 250 µg/mL, in an inhibition diameter of about 16.3–23 mm.[8] However, compared with fatty acids from *Ulva rigida*, (E)-17-(8-ethyl-4,5,9-trimethyldec-6-en-2-yl)-13-methyl-2,3,4,7,8,9,10,11,12,13,14,15,16,17-tetradecahydro-1H-cyclopenta[a]phenanthren-3-ol from *B. nitida* is less effective for microbes. It is necessary to develop the potential of the active group as a suitable alternative for dealing with infections.

The proliferation assay result showed that (E)-17-(8-ethyl-4,5,9-trimethyldec-6-en-2-yl)-13-methyl -2,3,4,7,8,9,10,11,12,13,14,15,16,17-tetradecahydro-1H-cyclopenta[a]phenanthren-3-ol had a better activity on MCF-7 cells with IC_{50} value of 142.18 µg/mL, compared to compound 1, with IC_{50} value of 681.65 µg/mL. From the results of the previous study, it was found that the ethyl acetate extract had a cytotoxic effect on HeLa cells of 281.09 µg/mL.[9] Green algae with cytotoxic activity include *Chaetomorpha bracyhygona* containing dichloacetic, oximes, and L-α-Terpinol as cytotoxic agent against SiHa cells with IC_{50} 23.6 µg/mL.[3] Another green algae is *Caulerpa lentifera* extract and fractions against various cells (100.50–7080.00 µg/mL), but in MCF-7 cells, the most effective was ethanol extract obtained using the maceration method with an IC_{50} value of about 100.9 µg/mL.[7,14] This study presents the potential of the active compound for further development as an anticancer agent. Based on the results, (E)-17-(8-ethyl-4,5,9-tri-methyldec-6-en-2-yl)-13-methyl-2,3,4,7,8,9,10,11,12,13,14,15,16,17-tetradecahydro-1H-cyclopenta[a]phenanthren-3-ol had moderate cytotoxic activity, and might be developed as an anticancer agent. The cell morphology was also observed to predict the mechanism of action for further studies. The photograph of MCF-7 cells treated with (E)-17-(8-ethyl-4,5,9-trimethyldec-6-en-2-yl)-13-methyl-2,3,4,7,8,9,10,11,12,13,14,15,16,17-tetradecahydro-1H-cyclopenta[a]phenanthren-3-ol showed blebbing suggesting apoptotic occurrence (Figure 5).

Considering MCF-7 cells were treated with (E)-17-(8-ethyl-4,5,9-trimethyldec-6-en-2-yl)-13-methyl -2,3,4,7,8,9,10,11,12,13,14,15,16,17-tetradecahydro-1H-cyclopenta[a]phenanthren-3-ol, programmed death was pre-dicted through observation of cells morphology. Simulation of the interaction with the caspase 3 receptor (Figure 6) was also conducted using molecular docking. The IC_{50} value of sitosterol 3β tetracosanoate was compared using in silico simulation. The binding energies and inhibition constant of (E)-17-(8-ethyl-4,5,9-trimethyldec-6-en-2-yl)-13-methyl -2,3,4,7,8,9,10,11,12,13,14,15,16,17-tetradecahydro-1H-cyclopenta[a]phenanthren-3-ol were lower than those of sorafe-nib and nature ligand (Table 3). The binding energy of sitosterol 3β tetracosanoate was larger than that of the sorafenib and the nature ligand. The potency of the inhibitory compound in blocking a receptor's function is indicated by the inhibition constant. A lower inhibition constant value indicates a greater inhibitory efficacy.[15] Meanwhile, a higher negative (lower) value indicates a good binding energy. A low binding energy indicates a higher possibility for interaction and the creation of a strong bond with the target protein, implying that the molecule needs less energy to bind.[16] Therefore, it can be clarified that the in silico and in vitro results are consistent. There is a crucial need to investigate the molecular mechanism and in vivo effects of (E)-17-(8-ethyl-4,5,9-trimethyldec-6-en-2-yl)-13-methyl -2,3,4,7,8,9,10,11,12,13,14,15,16,17-tetradecahydro-1H-cyclopenta[a]phenanthren-3-ol before the development as a therapeutic agent.

Conclusion

In conclusion, the green algae *B. nitida* contained sitosterol 3β tetracosanoate and (E)-17-(8-ethyl-4,5,9-trimethyldec-6-en-2-yl)-13-methyl-2,3,4,7,8,9,10,11,12,13,14,15,16,17-tetradecahydro-1H-cyclopenta[a]phenanthren-3-ol. Based on the results, (E)-17-(8-ethyl-4,5,9-trimethyldec-6-en-2-yl)-13-methyl-2,3,4,7,8,9,10,11,12,13,14,15,16,17-tetradecahydro -1H-cyclopenta[a]phenanthren-3-ol is a potential antimicrobial with an inhibition zone against *S. aureus* of 10.7 mm and an anticancer agent with the IC_{50} of 142.18 µg/mL. This is supported by in silico analysis, which (E)-17-(8-ethyl-4,5,9-trimethyldec-6-en-2-yl)-13-methyl-2,3,4,7,8,9,10,11,12,13,14,15,16,17-tetradecahydro-1H-cyclopenta[a]phenanth-ren-3-ol provides binding energy of −6.65 kcal/mol and inhibition constant of 13.46 µM. From the results obtained, (E)-

17-(8-ethyl-4,5,9-trimethyldec-6-en-2-yl)-13-methyl-2,3,4,7,8,9,10,11,12,13,14,15,16,17-tetradecahydro-1H-cyclopenta [a]phenanthren-3-ol has potential as an antimicrobial and anticancer agent. Further studies on the mechanism of action and in vivo tests are needed.

Acknowledgments

Disclosure

The authors declare that there are no conflicts of interest in this work.

References

1. Schindler K, Zobi F. Anticancer and Antibiotic Rhenium Tri- and Dicarbonyl Complexes: current Research and Future Perspectives. *Molecules*. 2022;27(2):539. doi:10.3390/molecules27020539
2. Gulumbe BH, Sahal MR, Abdulrahim A, et al. Antibiotic resistance and the COVID-19 pandemic: a dual crisis with complex challenges in LMICs. *Health Sci Rep*. 2023;6(9):e1566. doi:10.1002/hsr2.1566
3. Bray F, Laversanne M, Sung H, et al. Global cancer statistics 2022: GLOBOCAN estimates of incidence and mortality worldwide for 36 cancers in 185 countries. *CA Cancer J Clin*. 2024;74(3):229–263. doi:10.3322/caac.21834
4. Sleightholm R, Neilsen BK, Elkhatib S, et al. Percentage of Hormone Receptor Positivity in Breast Cancer Provides Prognostic Value: a Single-Institute Study. *J Clin Med Res*. 2021;13(1):9–19. doi:10.14740/jocmr4398
5. Paul S, Kundu R. Antiproliferative activity of methanolic extracts from two green algae, Enteromorpha intestinalis and Rizoclonium riparium on HeLa cells. *Daru*. 2013;21(1):72. doi:10.1186/2008-2231-21-72
6. Majumder I, Paul S, Nag A, Kundu R. Chloroform fraction of Chaetomorpha brachygona, a marine green alga from Indian Sundarbans inducing autophagy in cervical cancer cells in vitro. *Sci Rep*. 2020;10(1):21784. doi:10.1038/s41598-020-78592-9
7. Nurkolis F, Taslim NA, Qhabibi FR, et al. Ulvophyte Green Algae *Caulerpa lentillifera*: metabolites Profile and Antioxidant, Anticancer, Anti-Obesity, and In Vitro Cytotoxicity Properties. *Molecules*. 28(3):1365. doi:10.3390/molecules28031365
8. Ismail A, Ktari L, Romdhane YBR, et al. Antimicrobial Fatty Acids from Green Alga *Ulva rigida* (Chlorophyta). *Biomed Res Int*. 2018;2018:3069595. doi:10.1155/2018/3069595
9. Soekamto NH, Bahrun Okino T, Rasyid H, Pudjiastuti P, Hadisaputri YE, Zainul R. Chemotherapeutic prospects of organic extracts of Bornetella nitida from Selayar Island. *Kuwait J Scien*. 2024;51(3):1–8. doi:10.1016/j.kjs.2024.100223
10. Cayme J, Ragasa C. Structure elucidation of -stigmasterol and -sitosterol from Sesbania grandiflora (Linn.) Pers. and -carotene from *Heliotropium indicum* Linn. by NMR spectroscopy. *KIMIKA*. 2004;20(1112):5–12.
11. Ragasa C, Santosa VA, Shen C. Chemical Constituents of Moringa oleifera Lam. Seeds. *Int J Pharm Phytochemi Res*. 2016;8(3):495–498.
12. Sheikh YM, Kaisin M, Djerassi C. Steroids from starfish. *Steroids*. 1973;22(6):835–850. doi:10.1016/0039-128x(73)90057-3
13. Bahrun OT, Rasyid H, Soekamto NH. Biological evaluation and molecular docking of Indonesian *Gracilaria salicornia* as antioxidant agents. *J Pharm Res*. 2023;27(1):207–220. doi:10.29228/jrp.304
14. Mert-Ozupek N, Calibasi-Kocal G, Olgun N, Basbinar Y, Cavas L, Ellidokuz H. An Efficient and Quick Analytical Method for the Quantification of an Algal Alkaloid Caulerpin Showed In-Vitro Anticancer Activity against Colorectal Cancer. *Mar Drugs*. 2022;20(12):757. doi:10.3390/md20120757
15. Garcia-Molina F, Teruel-Puche JA, Rodriguez-Lopez JN, Garcia-Canovas F, Muñoz-Muñoz JL. The Relationship between the IC50 Values and the Apparent Inhibition Constant in the Study of Inhibitors of Tyrosinase Diphenolase Activity Helps Confirm the Mechanism of Inhibition. *Molecules*. 2022;27(10):3141. doi:10.3390/molecules27103141
16. Rena SR, Nurhidaya N, Rustan R. Analisis Molecular Docking Senyawa Garcinia mangostana L Sebagai Kandidat Anti SARS-CoV-2. *Jurnal Fisika Unand*. 2022;11(1):82–88. doi:10.25077/jfu.11.1.82-88.2022